

Risk of Hunger Under Climate Change, Social Disparity, and Agroproductivity Scenarios

Masanobu Kii · Keigo Akimoto · Ayami Hayashi

Received: 23 May 2011 / Accepted: 6 November 2012 / Published online: 8 December 2012
© Springer Science+Business Media Dordrecht 2012

Abstract Considering the projected population growth in the twenty-first century, some studies have indicated that global warming may have negative impacts on the risk of hunger. These conclusions were derived based on assumptions related to social and technological scenarios that involve substantial and influential uncertainties. In this paper, focusing on agrotechnology and food access disparity, we analyzed food availability and risk of hunger under the combined scenarios of food demands and agroproductivity with and without climate change by 2100 for the B2 scenario in the Special Report on Emissions Scenarios. The results of this study suggest that (1) future food demand can be satisfied globally under all assumed combined scenarios, and (2) a reduction of food access disparity and increased progress in productivity are just as important as climate change mitigation for reducing the risk of hunger.

Keywords Food availability · Agriculture · Climate change · Food access disparity · Crop productivity

1 Introduction

Climate change is considered to have an impact on food security. As stated in the Fourth Assessment Report by the IPCC [1], some studies support the premise that “stabilization of CO₂ concentrations reduces damage to crop production in

the long term,” therefore, “climate change is likely to increase the number of people at risk of hunger compared with reference scenarios with no climate change.” Past studies report a wide range of risk projections that depend on the assumed climate change and socioeconomic scenarios. However, the results may also depend on the prospect of agricultural technologies and more detailed socioeconomic situations such as food access disparity. These in-depth assumptions regarding food security have not yet been sufficiently addressed to assess the significance of factors other than climate change. In this study, we attempt to demonstrate the impact of future agroproductivity and food access disparity on food availability to contribute to the discussions of the risk of hunger under climate change.

Nelson et al. [2] have demonstrated the impact of climate change on the global production of selected crops under the A2 scenario in the Special Report on Emissions Scenarios (SRES) [3] towards 2050 using a global agricultural supply-and-demand projection model [4] linked to a biophysical crop model [5]. Compared with no climate change, under a climate change scenario, the world production of wheat and rice in 2050 is estimated to be lower by 23–27 and 12–14 %, respectively. Consequently, calorie availability in the developing world in 2050 is estimated to be lower than the availability in 2000, and the prevalence of child malnutrition will be 20 % higher. Based on that analysis, they concluded that agriculture and human well-being will be negatively affected by climate change.

Fisher et al. [6] applied a comprehensive assessment of agro-ecosystems and the agro-economy to estimate the impact of climate change on food security. This method combined the agro-ecological zone (AEZ) model [7] and the Basic Linked System (BLS) [8] to assess future food availability, taking into consideration climate scenarios, crop production, and socioeconomic drivers, as well as world food trade. Four emission and socioeconomic scenarios, known as the SRES A1, A2,

M. Kii (✉)
Faculty of Engineering, Kagawa University, 2217-20 Hayashi-cho,
Takamatsu, Kagawa 761-0396, Japan
e-mail: kii@eng.kagawa-u.ac.jp

K. Akimoto · A. Hayashi
Research Institute of Innovative Technology for the Earth,
9-2 Kizugawadai,
Kizugawa, Kyoto 619-0292, Japan

B1, and B2 (see Appendix I), were applied in the analysis. The results indicated that the impact is highly dependent on the scenarios, but that climate change is estimated to have an especially negative impact on poor developing countries. Using the same approach, Tubiello and Fisher [9] examined a modified A2 scenario by the International Institute of Applied Systems Analysis (IIASA) [10]. This scenario assumes a similar climate change as the original A2 scenario, but the population and gross domestic product are modified. Mitigation actions that reduce the climate impact are estimated to reduce the risk of malnutrition by 80–95 % compared with the non-mitigation case—this is due to the smaller production loss as a result of the action in less developed countries.

These studies have quantitatively clarified the possible impact of climate change on agriculture, taking into consideration the population and economic scenarios in SRES. However, other factors, such as technological progress and social disparity, have not yet been sufficiently studied. Agrotechnology appears to be incorporated in the BLS as external input, but how much the technological factor improves future crop yield was not described. The number of undernourished people was estimated as a function of the ratio of food supply over food requirement in those studies. If food allocation is completely equal, the share of undernourished people is zero when the supply/requirement ratio equals one. The undernourished share is illustrated as a declining curve over the food supply/requirement ratio in the above studies; the undernourished share falls below 20 % for the ratio of approximately 1.3 and almost zero for the ratio of higher than 1.6 in the study by Fisher et al. [6]. This means that inequity or disparity in food access is implicitly assumed in the relationship. Applying a fixed relationship in future estimation means that the disparity is also unchanged during the estimation period.

Agrotechnologies, including irrigation, fertilizers, and pesticides, as well as the development of new, more productive crop varieties through breeding or biotechnology, are considered to be major contributors to food security during the predicted population growth under the constraints of land, water, energy, and greenhouse gas emissions [11]. For instance, the global yield of wheat has increased approximately threefold between 1961 and 2008 [12]. This is considered to be an achievement of agrotechnological progress, including the chemical synthesis of nitrogen fertilizer. Wise et al. [13] conducted a sensitivity experiment related to the impact of crop productivity growth on terrestrial carbon emissions. Compared with their baseline productivity improvement, a frozen productivity scenario that made crop productivity constant at the 2005 level brought about an additional 70 PgC carbon emission from land use over the twenty-first century as a result of massive cultivation to meet increased food demand without yield improvement. Even though the assumption of frozen productivity is unrealistic, this experiment suggests the importance of the in-

depth prospect of the agrotechnological effect on food productivity in food security analysis.

Food security consists not only of food availability but also of access to and use of food [14, 15], as well as its stability [16]. In terms of food access, the demand side conditions, which include the growth of the real income of consumers, is expected to become more important over the next 50 years [17], even if enough food can be produced to feed the future population. As mentioned in studies of climate impact on food availability [6, 9], the elimination of malnutrition requires a higher food supply than the total dietary energy requirement because accessibility to food varies among people. These results suggest that greater elaboration in the assessment of the social side of food security is needed.

In this study, the impact of future agroproductivity and food access disparity on food availability is demonstrated using AEZ methodology combined with a global food demand and trade model. We assume four combined scenarios of possible disparities and agroproductivity with and without climate change by 2100 for the B2 scenario of the SRES. We consider that the B2 scenario is the most probable of the four scenarios, taking into account the recent demographic and economic trends. Based on these results, the impact of disparity reduction and the progress of agroproductivity compared with climate change mitigation on global food security are discussed.

2 Analysis Framework

For an impact assessment of food disparity and agroproductivity on food availability that takes climate change into consideration, we developed an analytical framework that consists of a global food system model and a grid-based agricultural land use model (Fig. 1). In this framework, regional food demand is estimated based on the GDP and

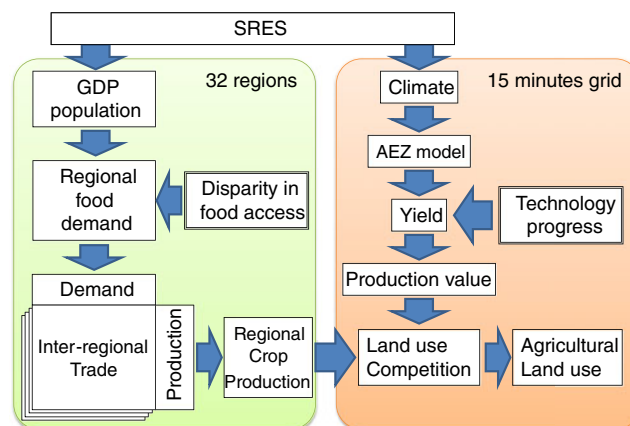


Fig. 1 Food availability assessment analytical framework

the population from SRES as well as the disparity scenario, which is discussed in section 4. Regional crop production to meet food demand is allocated based on an inter-regional trade model. Crop productivities are estimated using the AEZ model under the climate and agroproductivity progress scenarios. The productivities determine the possible production value of each land grid's crop when crop prices are given. The cropping grids are allocated to maximize the total production value of the region under the constraint of regional production volume given by the demand-trade model.

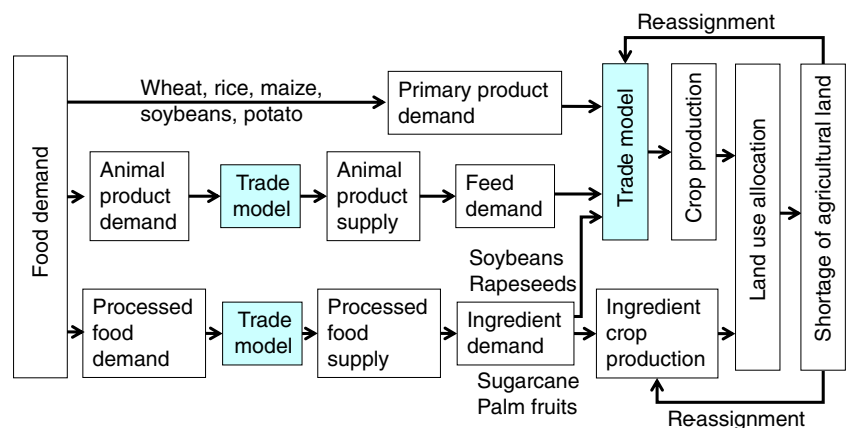
In this study, we assume 13 food items for final demand: wheat, rice, maize, soybeans, and potato as primary products; beef, pork, chicken, and milk as animal products; and sugar, soybean oil, rapeseed oil, and palm oil as processed food. In addition to the five primary products, sugarcane, rapeseed, and palm fruit are assumed as harvested crops. To meet world demand, the total agricultural land use allocation for eight kinds of crops is estimated. Feed for animal production is also assumed to consist of these eight kinds of crop, whose share is given based on the current share by region (see Appendix II). Processed food production requires an ingredient input of a corresponding crop. We assume that the ingredient in sugar is sugarcane, in soybean oil is soybean, in rapeseed oil is rapeseed, and in palm oil is palm fruit. All of the food items and crops are tradable among regions except for sugarcane and palm fruit because these two crops quickly deteriorate, which makes inter-regional trade difficult. Regional demand is satisfied by domestic and imported products, and the share of domestic product is calculated by a binary logit model [18] using the domestic and import price. Imports of all regions are aggregated into global trade demand, and the export share in the international market is calculated by a multinomial logit model using the prices of export regions. The details of this trade model are described in Appendix III. All data required for the model estimation were obtained from FAOSTAT [12]. Even though trade is defined by the model, because we fixed the prices of all regions and crops for future estimation, the share of domestic product or the international market is constant except in the case where there is an agricultural land

shortage, which is described below. The estimation process from food demand to agricultural land use allocation is shown in Fig. 2.

For food demand, trade, and crop production estimation, the world is divided into 32 regions, considering socioeconomic cohesiveness, geographical adjacency, and integrality of the food market (Fig. 3). To meet the estimated regional food production, agricultural land use is allocated on a 15 × 15 min land grid. One allocated grid is fully used for the production of one selected crop. The harvested crop is selected to maximize the grid's production value, considering the yields estimated by the AEZ model and given producer prices for all crops. The crops are allocated to meet the estimated regional crop production. If there is a shortage of agricultural land, the production shortage is reallocated through the trade model to regions where agricultural land remains. In the simulations, the available agricultural land is initially limited to the cropland grid in the USGS land use datasets [19], but is expanded to adjacent grids for the regions where agricultural land shortage occurred in the previous period.

It should be noted that the crop demand for energy use is not incorporated in this study. The global production of ethanol is increasing, from 17.3 billion liters in 2000 to over 46 billion liters in 2007, and it is expected to exceed 125 billion liters in 2020 with worldwide government programs [20]. However, the current production cost of bioethanol is much higher than that of fossil fuel, except for the bioethanol from sugar cane in Brazil [21]. This means that supporting policies or regulations are needed to promote bio-energy use and production. Competition between energy and food provision would raise concerns in producing biofuels from food crops [22]. For instance, the promotion of bioethanol production from maize in the USA began as a countermeasure for oversupply [23]. It is uncertain whether the promotion of biofuel would last long under a situation of tight supply of ingredient crops and competition with food. An increase in the use of food crops for energy production will affect agricultural production, price, and risk of hunger.

Fig. 2 Estimation process for agricultural land use allocation



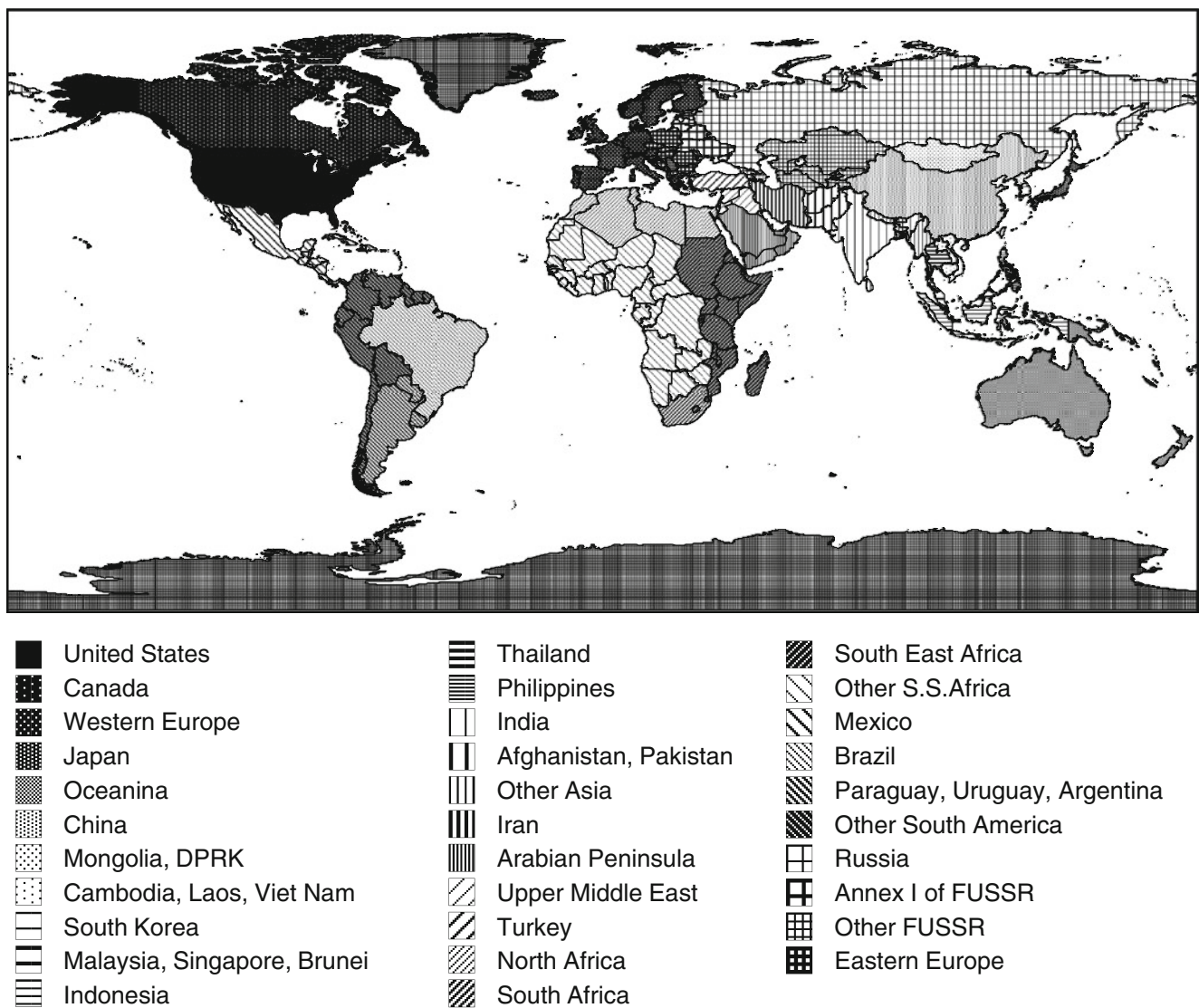


Fig. 3 Thirty-two regions for demand, trade, and crop production estimation

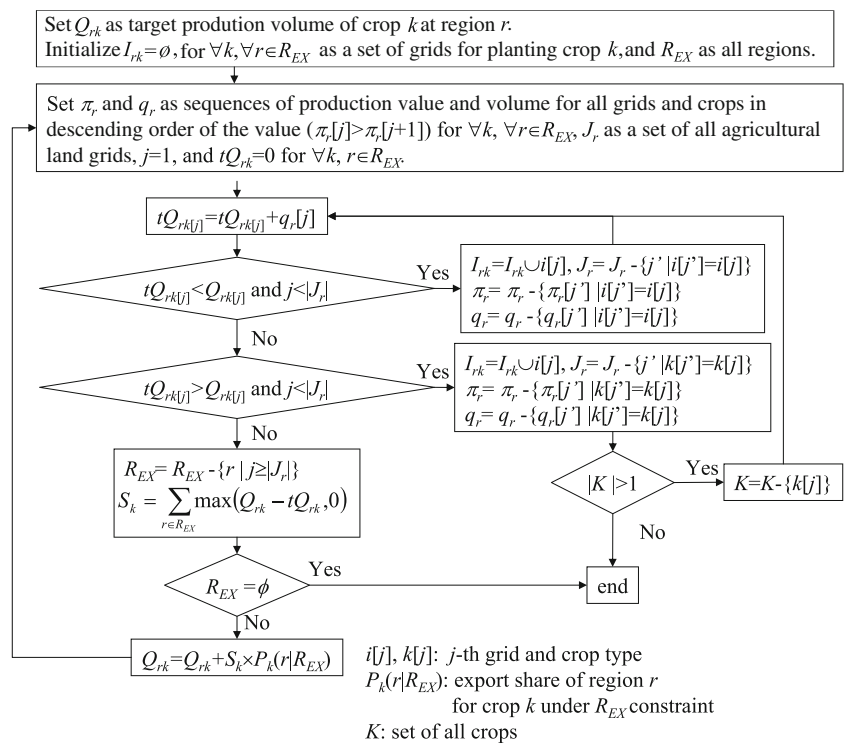
However, we did not include crop production for energy use in this study because of the uncertainties around the future demand for biofuels.

Figure 4 shows the estimation algorithm for agricultural land use. First, we set Q_{rk} as the target production volume of crop k in region r derived from the food demand and trade model. We also initialized π_r and q_r as sequences of the production value and volume for all grids and crops in region r in descending order of production value. This means that $\pi_r[j] > \pi_r[j+1]$, where $\pi_r[j]$ represents the j th production value in the sequence π_r . J_r is a set of j , which is a sequence of all combinations of land grids and crops in region r . Temporary production volume is denoted as tQ_{rk} and set as $j=1$ and $tQ_{rk}=0$ as the initial value.

For each region, the temporary production volume of crop $k[j]$ is set to $tQ_{rk[j]} = tQ_{rk[j]} + q_r[j]$, where $k[j]$ denotes the j th crop in the production value sequence. This means

that the grid that gives the highest production value is selected to harvest crop k . If $tQ_{rk[j]} < Q_{rk[j]}$ and $j < |J_r|$, as shown in the first branch, we add grid $i[j]$ to I_{rk} , which is a set of grids where crop k is harvested in region r . In this case, the grid cannot be used to harvest another crop. Therefore, j' , which indicates the same grid as j (i.e., $i[j'] = i[j]$) but harvests another crop, has to be removed from J_r . In the same way, the data of production value and volume indicating grid $i[j]$ in the sequence π_r and q_r are also removed. If $tQ_{rk} > Q_{rk}$ and $j < |J_r|$, as shown in the second branch, this means that the temporary production exceeds the target production and there is still room for production, but no more grids for producing crop k are needed. In this case, therefore, we add $i[j]$ to I_{rk} and remove all data for the crop k from J_r , π_r , and q_r . Here, if there are other crops for which the temporary production volume is less than the target volume, we remove the crop k from the set of crops

Fig. 4 Algorithm for agricultural land use allocation



K . Otherwise, if all temporary production volumes exceed the target volumes, this algorithm ends. If $j > |J_r|$, which means that no grids are left for cultivation, region r is removed from R_{EX} and the shortage of production S_k is set as the difference between the target and the temporary production volume. If R_{EX} is not empty, the shortage is reallocated to the target volume Q_{rk} in the regions of R_{EX} through the trade model that gives the export share $P_k(r | R_{EX})$. If R_{EX} is empty, algorithm stops and the output is the total shortage of all crop productions.

In this framework, the estimated global agricultural land use allocation is consistent with food demand and crop yields under the socioeconomic, climate, and agroproductivity conditions. For agricultural land use projection during the twenty-first century, SRES provides greenhouse gas emission paths and basic socioeconomic conditions. Based on the emission path, general circulation models calculate long-term grid-based global climate conditions that are inputs of the AEZ model to estimate the crop yield in each grid. As technological factors for yield estimation in the AEZ model, Leaf Area Index and Harvest Index are incorporated; they are represented as coefficients for the gross and net biomass production estimation, and those values are given by three input categories. For the projections, therefore, the yield depends on the choice of input category, but there are no standard methods for how to choose one. In addition, AEZ estimates the possible yield in each grid cell, but it does not give information in regard to where each crop is harvested and how much of the crops are produced in regions.

Relationships among population, GDP, and average food demand can be captured statistically using the FAOSTAT data [12] of past decades. However, this statistical relationship does not necessarily reflect the disparity in food access and malnutrition of poverty groups. SRES can provide an average income index as per-capita GDP, but it does not give its distribution. As mentioned in Section 1, past studies projecting the impact of climate change on food security implicitly assumed a distribution and did not consider a change in disparity.

A comparison with Computable General Equilibrium (CGE) models coupled to agricultural land use models [24–26] would be helpful to understand the features of our approach. The Global Trade Analysis Project (GTAP) model [27] is often used as a CGE model for the analysis of the effect of climate change on global agriculture and land use. CGE models are based on the Walrasian perfect competition paradigm to generate a general equilibrium state where the supply and demand of all markets in the economic system are balanced by adjusting the prices. Actors in the model, firms and households, behave to maximize their profit and utility at a given price under the resource constraints. In the GTAP model, there are multiple industrial sectors and the world is divided into multiple regions. The model represents the interregional trade of all commodities including agricultural products. In this model, the demand and supply of food are elastic to the prices, and the interregional trade is flexible, and will change according to resource constraints, especially land use. Some studies define land constraints by agricultural land use models such as the AEZ model.

On the other hand, in our approach, the final food demands are initially determined based on the regional per capita income, then supply volume is allocated to the regions using their current trade share, and finally land use to meet the given production volume is assigned to grids in each region. This means that food demand is inelastic to price, and that the import/export share is fixed to the current level except in the case of land use shortage for food provision. Therefore, our approach can be described as an analysis of the physical availability of food supply under the expected food demand and current trade system.

Food demand and trade are probably affected by price, which is determined by the market under perfect competition, as assumed in CGE models. However, in our *ex ante* analysis using the FAO database, we could not find significant relationships among food price, demand, trade, and production that consider the tariff and subsidy of each region. In other words, we could not capture the effect of price on food consumption or production from historical data. Both demand and supply of agricultural products may reflect not only its price but also other factors such as preference, regulation, and the distribution system. International trade may depend on the bilateral political or cultural relationships. If the relationships among price, demand, trade, and production are clarified, our model can be easily expanded to a partial equilibrium model that limits the sectors in CGE to agriculture. A further calibration study is needed.

In the next section, the technological factor for regional yield estimation is addressed, and a food demand scenario considering food access disparity is discussed in Section 4.

3 Estimation of the Agrotechnological Factor and its Future Scenarios

In this section, we introduce the agrotechnological factor to clarify the method to generate the agroproductivity scenarios. To estimate yields that are consistent with their statistics, harvested land grids for each crop have to be specified. For that task, we use the agricultural land use allocation algorithm shown in the previous section. In the application of this algorithm, the target production volume for each crop and region is given by FAOSTAT for the year to be calibrated. Once the harvested grids are determined, while the grid allocation procedure requires the yields of each grid, the average yield in the region can be obtained. The agrotechnological factor is adjusted to fit the estimated regional average yield with its statistics under the regional production constraint, but the yield adjustment will change the land use allocation that affects the average yield. Therefore, this adjustment process has to be iterative.

We simply determine the agrotechnological factor as a multiplicative coefficient of the original AEZ yield estimation,

and determine the actual yield as a product of the agrotechnological factor and the AEZ yield. We denote the AEZ yield with moisture content for grid i and crop k as Y_{ki}^{AEZ} , actual yield as Y_{ki} and the agrotechnological factor as H_k , which is region- and crop-specific, then $Y_{ki} = H_k \times Y_{ki}^{AEZ}$. Using Y_{ki} , a set of harvested grids I_k , and area of grid i A_i , the total production volume of crop k in region Q_k can be expressed as follows:

$$Q_k = \sum_{i \in I_k} Y_{ki} \cdot A_i \quad (1)$$

The regional average yield Y_k is estimated as follows:

$$Y_k = Q_k / \sum_{i \in I_k} A_i \quad (2)$$

If I_k was fixed, the agrotechnological factor H_k' , which makes the estimated yield identical to that in statistics Y_k^* could be calculated using the following equation:

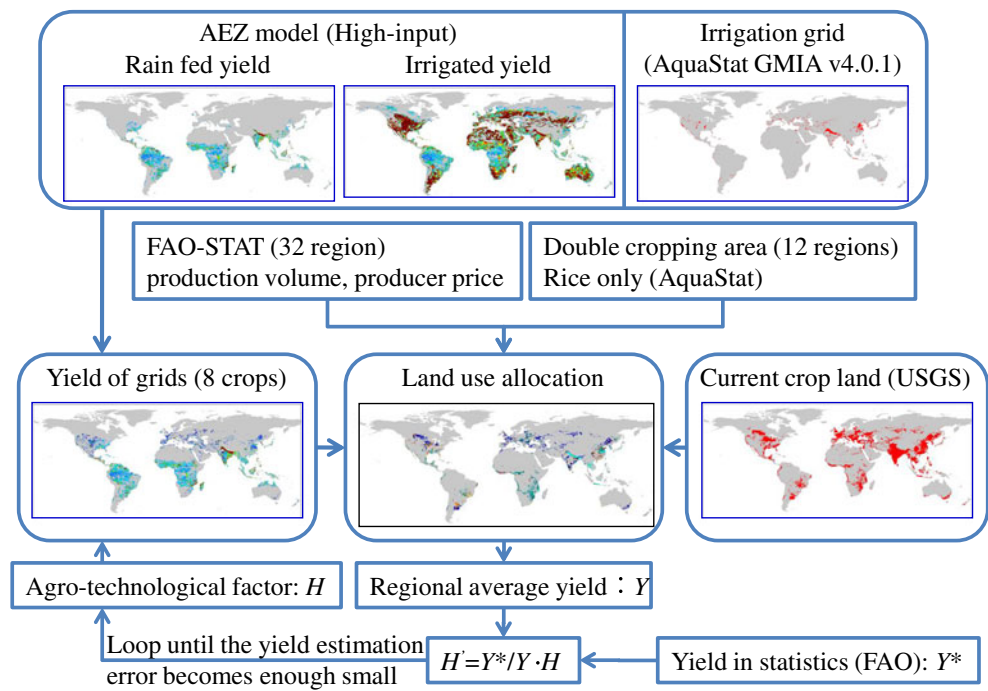
$$H_k' = H_k \cdot Y_k^* / Y_k \quad (3)$$

I_k will change if H_k is updated because this adjustment changes the production value of corresponding crops in each grid that affect the land use competition among crops; therefore, I_k must be updated through the land use allocation algorithm. In summary, H_k and I_k are calculated alternately until the error of the yield estimation for every crop is small enough. This estimation flow is shown in Fig. 5.

The estimated AEZ yield in this study reflects the current climate (monthly temperature, precipitation, cloud cover, wind speed, and humidity), soil condition [8], slope/height [28], and irrigation. Grid climate conditions are estimated based on the CRU dataset [29] and pattern scaling method [30] using MIROC 3.2 medres, which was obtained from a database by the Program for Climate Model Diagnosis and Intercomparison [31]. The irrigated grids are given based on the AQUASTAT database [32] and both rain-fed and irrigated yields are calculated using the AEZ model. Irrigated yields are applied to irrigated grids, and rain-fed yields are applied to the other grids. Based on the AQUASTAT database, double cropping grids of rice are also estimated. AQUASTAT also gives double cropping areas for rice, and we assume that double cropping grids are allocated to a higher yield grid so that the regional total area of the grids equals the statistics. In addition, land use allocation is limited to the current crop land grid, which is compiled based on the USGS database [19] for the current agrotechnological factor estimation.

Applying this procedure to estimate the agrotechnological factor for four periods, 1990, 1995, 2000, and 2005, the correlation of regional yield between the estimation and statistics for every crop and period is no less than 0.98. The production target constraints are satisfied for all crops in each estimation, and therefore, the area harvested can also be accurately estimated using this factor.

Fig. 5 Flowchart of the agrotechnological factor estimation



For future productivity projections, the main concern is how to estimate the agrotechnological factor for each region. First, we considered that this factor somewhat reflects the input of agricultural technologies, which may correlate with the economic development of the region. Figure 6 plots agrotechnological factors vs. GDP per capita in 2,000 USD, considering cases of wheat, rice, and maize. The factor has a tendency to increase as per-capita GDP grows, but it varies widely even among both higher and lower income groups.

The agrotechnological variation probably reflects various regional backgrounds such as culture and food preferences, land use constraints, agricultural labor/capital conditions, and affordability/cost-effectiveness/policies on intensive farming. Some high-income regions seem to take on extensive farming and some low-income regions appear to intensively input agrotechnologies. In the future, an acceptance

of the use of biotechnologies, including genetically modified organisms or agrochemicals, may widen the difference in the factors among regions. Furthermore, it is quite uncertain which pathway would be taken by the current low-income and low-technology regions that are expected to have higher economic growth during this century.

For this reason, we simply apply autonomous yield increasing rates to the agrotechnological factor scenarios. The rates are estimated based on historical statistical data covering 43 years. To remove annual fluctuations, we take a 5-year moving average of both yield and its growth rate. Based on a nonparametric analysis, the average growth rate was found to tend to decline against its yield. Therefore, we assume that the average growth rate can be represented by an exponential function with input of yield ($f(Y) = \alpha_0 \exp\{\alpha_1 Y\}$; Y: Yield, α_0, α_1 : parameters). The

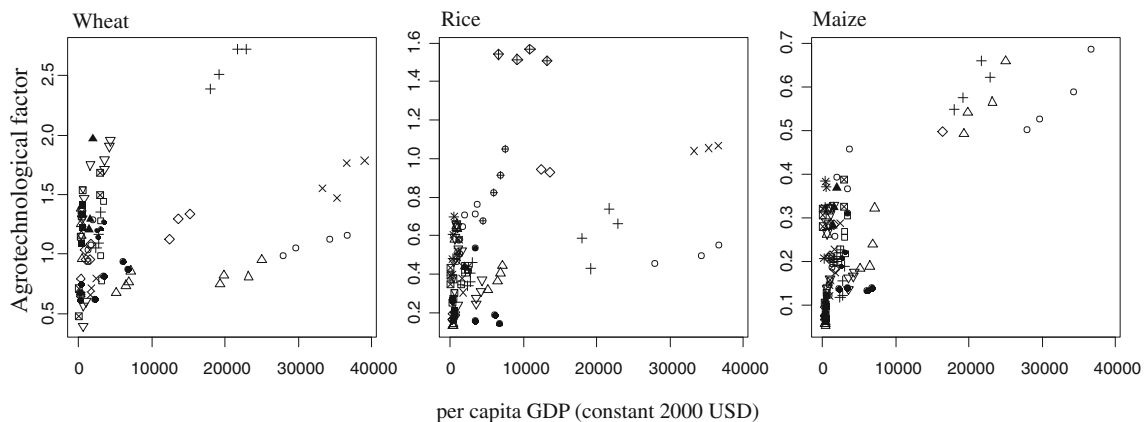


Fig. 6 Relationship between agrotechnological factors and per-capita GDP

parameters and their standard errors are estimated by the maximum likelihood method. In this study, we take two scenarios for the future growth rate; one is based on the expected parameter values and the other is based on the lower bound of parameters with 66 % confidence, assuming normal distributions for parameter errors.

Using these growth rate functions, agrotechnological factor scenarios are determined by the following equation:

$$H_{kr}^{t+1} = H_{kr}^t \cdot \{f(Y_{kr}^t) + 1\} \tag{4}$$

where Y_{kr}^t and H_{kr}^t are yield and agrotechnological factor of crop k in region r at year t , respectively. Figure 7 shows a plot of yield and its growth rate for wheat, and Fig. 8 shows the estimated agrotechnological factor scenarios for selected regions. In Fig. 7, the gray plot shows the observed yield and annual growth rate as a 5-year moving average, and the solid and dotted lines represent the functions with expected and lower bound parameters, respectively. The two charts in Fig. 8 depict estimated past agrotechnological factors (1990–2005) and their future scenarios (2010–2100) for five regions. In Fig. 7, the assumed two growth rate curves appear relatively close to each other when compared with the actual growth rate distribution (both of these two curves show the average growth rate, but one represents its expected average and the other shows the lower bound with 66 % confidence), but we can see that this slight variation generates a significant difference in the long-term productivity scenarios. In the lower growth scenario, the agrotechnological factor increases by 63 % on average for all crops and regions from 2005 to 2100, and by 151 % in the average growth scenario. In this study, we apply these growth curves as the technological scenarios. Of course, productivity by region will bring about a wider variety of scenarios because of regionality or fluctuations. Additionally, if we assume a higher confidence level, the range of scenarios will be wider.

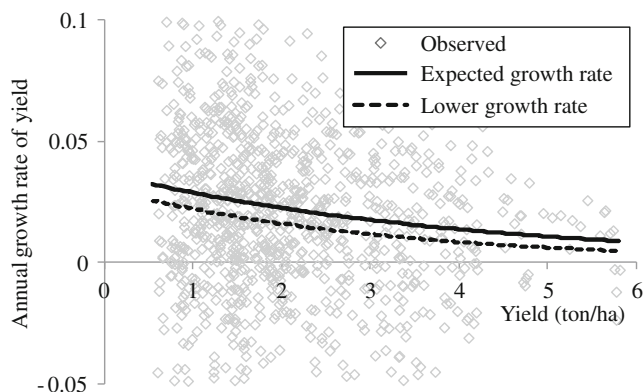


Fig. 7 Yield and growth rate for wheat

4 Disparity in Food Access

Food accessibility is an important component of food security, as discussed in Section 1. To evaluate food accessibility based on a food demand/supply analysis, we employ the estimation method and undernourishment prevalence data of the FAO Statistics Division [33]. In the FAO framework, the proportion of undernourished in the total population P_U is determined by the following equation:

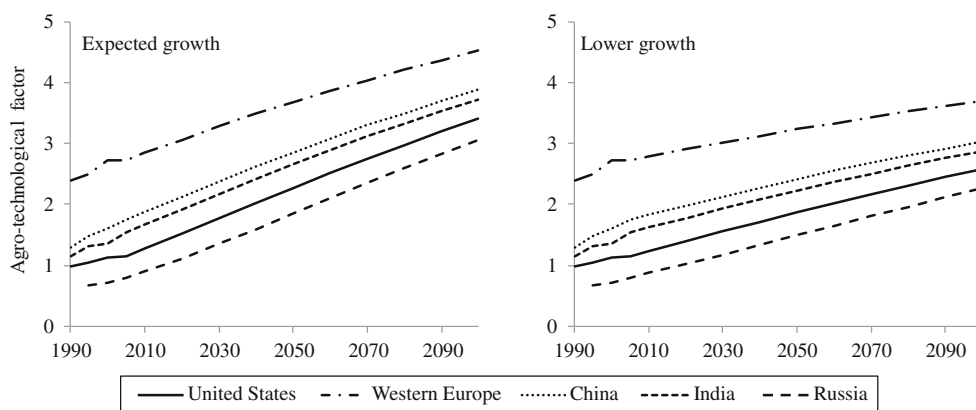
$$P_U = P(x < r_L) = \int_{x < r_L} f(x) dx \tag{5}$$

where x refers to dietary energy consumption, r_L is the minimum dietary energy requirement, and $f(x)$ is the density function of dietary energy consumption. Here, $f(x)$ is assumed as a lognormal density function with mean and deviation parameters μ and σ . These parameters are estimated by FAO based on a Food Balance Sheet and household budget survey in each country. With this framework, the FAO provides estimates of the prevalence of undernourishment in the total population and minimum dietary energy requirements on their website of food security statistics [34]. Though FAO does not publish the parameters of the density functions, they can be calculated using the above data.

Using the lognormal distribution parameter σ , the GINI coefficient of dietary energy consumption can be calculated [35]. Here, the degree of disparity of food access can be expressed by the GINI coefficient. This is one of the definitive factors of the prevalence of undernourishment. Therefore, its assumption is no less important than average food consumption for the food security analysis. For instance, the average food consumption and prevalence of undernourishment in India in 2004 are 2,473 kcal/capita/day and 21 %, respectively, and the minimum dietary energy requirement is 1,770 kcal/capita/day. Assuming a lognormal distribution in dietary energy consumption, its GINI coefficient is calculated as 0.19, as shown in Fig. 9a. To make the prevalence less than 5 % using the same GINI coefficient, the average energy consumption has to be more than 3,294 kcal/capita/day (Fig. 9b). Meanwhile, if the GINI coefficient is assumed to be 0.11, which is the minimum value in the FAO database [36], it takes an average consumption of 2,489 kcal/capita/day to make the prevalence of undernourishment 5 % (Fig. 9c). This example suggests that the alleviation of food access disparity would reduce the number of undernourished people significantly, with a relatively small increase in total food consumption. In contrast, if the disparity was unchanged, a substantial amount of food provision would be required to eliminate the malnutrition.

Based on the above discussion, we set two scenarios for future food demand: fixed and reduced food access disparity. In the fixed scenario, the GINI coefficient estimated from

Fig. 8 Agrotechnological factor scenarios for wheat



current average energy consumption and the prevalence of malnutrition in each region is used. The reduced scenario sets the GINI coefficients of all regions to the value 0.11, which is the minimum value given in the FAO database. We assume that chronic malnutrition is eliminated when the prevalence is less than 5 % (a value less than 5 % is represented by a dash mark in the FAO database), and define the average food consumption that eliminates malnutrition under a given GINI coefficient as the saturation level of food demand per

capita. Based on the GINI coefficient scenarios, two saturation levels are generated.

Table 1 presents the food access indices and parameters for these two scenarios in the 27 regions where the prevalence of malnutrition was less than or equal to 5 % in 2003. The values of the average food consumption and the prevalence of malnutrition in 2003 are also listed. In this table, the middle group of columns (GINI in 2003) shows the parameters estimates based on food access indices in 2003.

Fig. 9 Dietary energy consumption distribution and prevalence of undernourishment in India

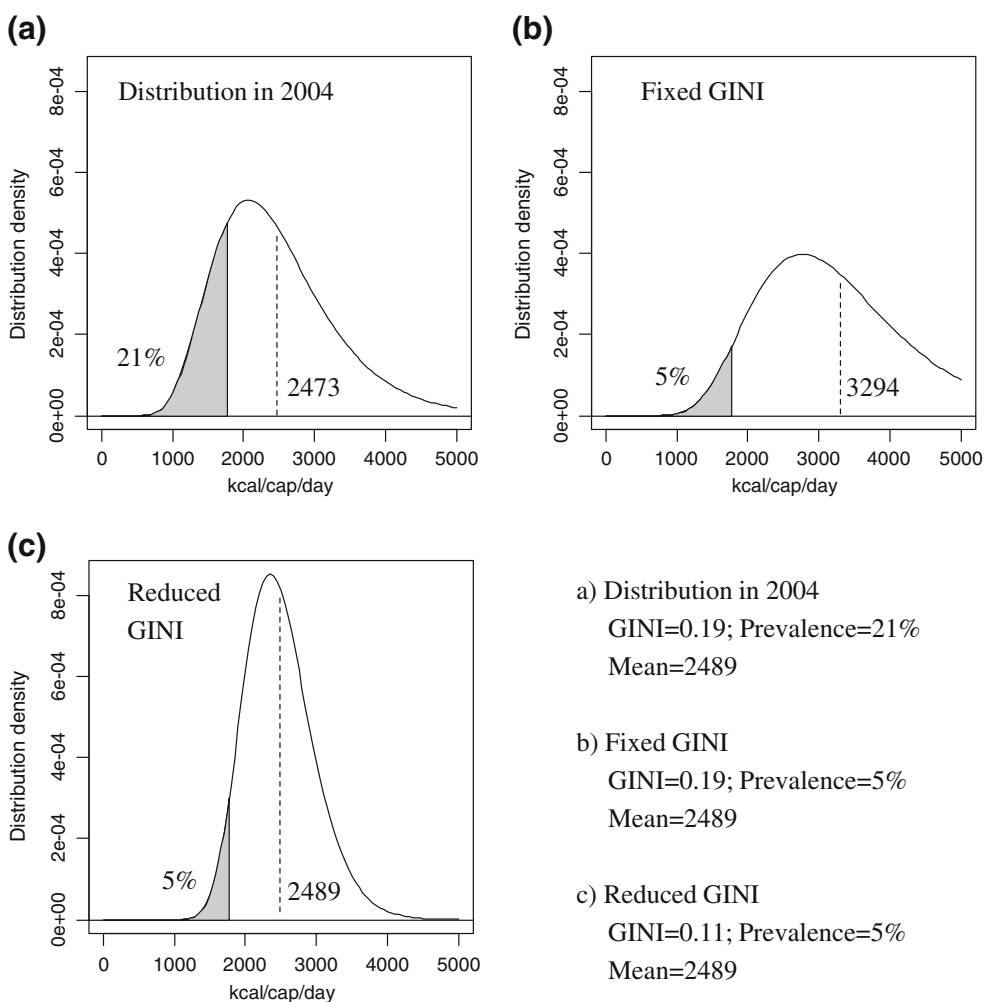


Table 1 Food access indices for the two food demand scenarios

Region	In 2003			Fixed GINI scenario (GINI in 2003)				Reduced GINI scenario (GINI=0.11)			
	Minimum dietary energy requirement (kcal/day)	Average food consumption (kcal/day)	Prevalence of malnutrition (%)	Log-scale mean	Log-scale s.d.	GINI ^a	Saturation level ^b	Log-scale mean	Log-scale s.d.	GINI ^a	Saturation level ^b
Oceania ^c	1,811	2,746	7	7.89	0.254	0.142	2,840	7.82			2,547
China	1,900	2,940	9	7.94	0.294	0.164	3,215	7.87			2,672
Mongolia, DPRK	1,858	2,186	32	7.65	0.266	0.149	2,984	7.85			2,613
Cambodia, Laos, Viet Nam	1,787	2,528	16	7.79	0.302	0.169	3,072	7.81			2,513
South Korea	1,900	3,035	5	7.98	0.264	0.148	3,035	7.87			2,672
Malaysia, Singapore, Brunei	1,811	2,867	5	7.93	0.259	0.145	2,867	7.82			2,547
Indonesia	1,810	2,891	17	7.89	0.405	0.225	3,824	7.82			2,545
Thailand	1,850	2,424	17	7.76	0.251	0.141	2,883	7.84			2,601
Philippines	1,750	2,480	16	7.77	0.304	0.170	3,023	7.79			2,461
India	1,770	2,473	21	7.75	0.342	0.191	3,294	7.80			2,489
Afghanistan, Pakistan	1,750	2,316	23	7.70	0.313	0.175	3,076	7.79			2,461
Other Asia	1,767	2,398	23	7.72	0.341	0.191	3,283	7.80			2,484
Iran	1,810	3,096	5	7.99	0.299	0.167	3,096	7.82			2,545
Arabian Peninsula	1,791	2,522	17	7.79	0.305	0.171	3,099	7.81	0.196	0.11	2,518
Upper Middle East	1,813	3,009	5	7.97	0.283	0.159	3,009	7.82			2,550
Turkey	1,920	3,328	5	8.06	0.306	0.171	3,328	7.88			2,700
North Africa	1,835	3,233	5	8.03	0.314	0.176	3,233	7.84			2,581
South East Africa	1,728	2,057	35	7.58	0.317	0.177	3,061	7.78			2,430
Other S.S.Africa	1,756	2,347	27	7.69	0.367	0.205	3,435	7.79			2,470
Mexico	1,831	2,897	10	7.92	0.323	0.180	3,280	7.83			2,575
Brazil	1,850	3,146	6	8.01	0.310	0.174	3,235	7.84			2,601
Paraguay, Uruguay, Argentina	1,879	2,901	6	7.94	0.255	0.143	2,950	7.86			2,642
Other South America	1,801	2,536	12	7.80	0.262	0.147	2,868	7.82			2,532
Russia	1,950	3,118	5	8.01	0.264	0.148	3,118	7.90			2,742
Annex I of FUSSR	1,940	3,047	5	7.99	0.255	0.143	3,047	7.89			2,728
Other FUSSR	1,887	2,553	13	7.82	0.240	0.135	2,884	7.86			2,653
Eastern Europe	1,967	3,257	5	8.05	0.282	0.158	3,257	7.91			2,766

S.S Africa denotes Sub-Saharan Africa, *FUSSR* Former Union of Soviet Socialist Republics

^a The estimated GINI coefficient of dietary energy consumption

^b The maximum level of average food consumption required to meet the condition that the prevalence of malnutrition equals 5 % under the given GINI coefficient

^c Oceania does not include Australia and New Zealand

Here, log-scale mean and standard deviation (s.d.) indicates the lognormal distribution parameters of food access disparity, and GINI is the GINI coefficient of dietary energy derived from the distribution. Saturation level indicates the average food consumption required to meet the condition that the prevalence of malnutrition equals 5 % under the given GINI coefficient (the assumed relationships between the average food consumption, per capita GDP and the saturation level are denoted in Eq. 6.). Therefore, for the regions whose prevalence of

malnutrition is equal to 5 % the average food consumption in 2003 value is taken.

The right group of columns (GINI=0.11) indicates the distribution parameters and saturation levels when the GINI coefficient is fixed to 0.11 for all regions. By definition, the same GINI coefficient requires the same standard deviation of the lognormal distribution, but its mean parameter differs depending on the minimum dietary energy requirement. This scenario assumes a smaller disparity in food access; therefore, the average food consumption (saturation level)

required to make the prevalence of malnutrition 5 % is smaller than that in the fixed GINI scenario.

Average food consumption and per capita GDP were found to be highly correlated in the data analysis, and we assumed the following logistic growth function for average food demand:

$$Q = \frac{\beta_3}{1 + \exp(\beta_1 \cdot \text{GDP} + \beta_2)} + (S - \beta_3) \quad (6)$$

where Q is average food demand (kcal/capita/day), GDP is per-capita GDP (constant 2000 USD), S is the saturation level, and β_1 , β_2 , and β_3 are parameters. Here, the parameters are estimated by the maximum likelihood method using time-series data of each region. However, five of the total 32 regions, the US, Canada, Western Europe, Japan, and South Africa, have less than 5 % of the prevalence of malnutrition in the database, and the saturation level S cannot be given by the food access disparity indices for these regions. These five regions are almost developed regions, and the average food demand looks nearly saturated. Therefore, $(S - \beta_3)$ in the above equation for these five regions is substituted by an additional parameter β_4 and is statistically estimated with other parameters. Here, the parameters for Canada were not estimated to be significant; therefore, we applied the US saturation level in Eq. 6 and estimates β_1 , β_2 , and β_3 for Canada.

The estimated values for the parameters in Eq. 6 are given in Tables 2 and 3. Figure 10 depicts the time-series data for dietary energy consumption and its estimation using the model assuming a fixed GINI coefficient for selected regions. For all regions in this figure, the model estimation has a good fit with observed data where the correlations between them are more than 0.9. Looking at China in this figure, the observed consumption is almost stable from 1998 to 2003, but the estimate still increases. This reflects the higher assumed saturation level than the current consumption level and the high economic growth during this period. Therefore, the consumption is possibly overestimated, but if the current prevalence of malnutrition is 9 %, as shown in the FAO database, and if it has to be less than 5 % in the saturation stage, the average consumption must increase. In this sense, the demand estimation is not just a projection based on a past trend but reflects the future target in the crusade against undernourishment.

Regarding the overall fitness of the model under the fixed GINI scenario, 16 regions have a correlation coefficient of more than 0.9; in five regions, it is between 0.7 and 0.9. The remaining 11 regions have relatively poor fit and they are mostly positioned as low developing regions, the Middle East, and Economies in Transition (EIT). For low developing regions, they remain in the starting stage of economic growth, and therefore, dietary energy consumption is not

necessarily explained by the economic index. In the Middle East, GDP is highly correlated with oil price, and hence, it is not an adequate index for representing the past consumption trend. In EIT regions, per capita dietary energy consumption was almost stable, but GDP declined in the 1990s, so the consumption cannot be explained by the per-capita GDP in the past.

Despite the poor fit of the models for these 11 regions, we apply them in future scenario building if the estimated model parameters satisfy sign conditions that represent a positive relationship between average dietary energy consumption and per-capita GDP. In addition, for the regions where the current energy consumption has already exceeded the determined saturation level, the future average dietary energy consumption is fixed to the saturation value in the scenario. As a result, three regions do not satisfy the conditions above and the parameters of adjacent regions are applied to them with modification to meet the given saturation level, in particular, the parameters of Iran, South East Africa, and Russia are applied to the Arabian Peninsula, other Sub-Saharan Africa, and other Former Union of Soviet Socialist Republics, respectively.

The generated per-capita dietary energy consumption scenarios are shown in Fig. 11. Here, the developed countries, the US, Western Europe, and Japan, have single saturation parameters, and therefore, their paths are the same in both scenarios. In contrast, developing regions have different pathways between the two scenarios. In the fixed GINI scenario, all of the developing regions exceed Japanese consumption. This is due to the higher saturation level of average energy consumption to meet the condition of a 5 % prevalence of malnutrition under high food access disparity, as shown in Table 2. Meanwhile, all of their average consumptions are below Japan in the reduced GINI scenario because of the lower saturation level under more equal food access, as shown in Table 3. In the latter case, China and Indonesia reduce their future consumption from the current level. We assume that malnutrition will be resolved even if the average dietary energy consumption declines because the food access disparity is greatly reduced.

Furthermore, we decompose these dietary energy consumption scenarios into the demand for the 13 food items described in Section 2. First, we defined four food classes: cereals and vegetables (wheat, rice, maize, soybeans, and potato), animal products (beef, pork, chicken, and milk), sugar, and oil (soybean oil, rapeseed oil, and palm oil). We assume that the share of animal products, sugar, and oil grows as per-capita GDP increases. The share of cereals and vegetables is calculated by subtracting the other shares from one. Again, a logistic function is applied as the share growth model. The shares of these classes in the USA, Western Europe and Japan have been almost stable during

Table 2 The estimated values for parameters of the food demand function (fixed GINI scenario)

Region names	Average consumption (kcal/day)	β_1	β_2	β_3	β_4	Saturation level (kcal/day)	Correlation
USA ^a	3,754	-0.19 (-7.15)	4.96 (7.29)	1,176.44 (10.06)	2,765 (48.71)	3,941	0.994
Canada ^b	3,605	-0.47 (-10.98)	10.33 (11.01)	1,036.61 (50.88)	-	3,941	0.964
Western Europe ^a	3,536	-0.09 (-1.67)	0.71 (0.54)	1,633.2 (1.39)	2,205 (2.31)	3,838	0.983
Japan ^a	2,768	-0.11 (-0.35)	-0.21 (-0.01)	1,240.77 (0.07)	1,583 (0.09)	2,824	0.952
Oceania ^a	3,114	0.00 (0.33)	-3.84 (-0.08)	-11,038.18 (-0.02)	-	2,840	0.057
China	2,940	-2.44 (-13.87)	-1.93 (-5)	13,008.19 (2.91)	-	3,215	0.972
Mongolia, DPRK	2,185	-5.64 (-0.5)	3.7 (0.64)	933.93 (4.24)	-	2,984	0.248
Cambodia, Laos, Viet Nam	2,530	-5.54 (-1.89)	1.96 (1.06)	1,400.02 (2.53)	-	3,072	0.978
South Korea ^c	3,035	-3.49 (-5.88)	5.32 (4.21)	1,073.25 (6.59)	-	3,035	0.980
Malaysia, Singapore, Brunei ^c	2,867	-0.76 (-5.43)	0.87 (0.89)	835.95 (2.31)	-	2,867	0.968
Indonesia	2,891	-1.5 (-37.58)	-1.07 (-4.24)	10,043.58 (5.15)	-	3,824	0.994
Thailand	2,424	-0.33 (-6.34)	-1.18 (-1.62)	3,734.12 (1.76)	-	2,883	0.835
Philippines	2,480	-3.48 (-2.49)	2.68 (1.34)	2,129.71 (2.22)	-	3,023	0.905
India	2,473	-2.16 (-7.66)	-0.68 (-1.16)	5,052.41 (2.48)	-	3,294	0.901
Afghanistan, Pakistan	2,316	-1.72 (-14.49)	-0.9 (-1.01)	4,753.95 (1.51)	-	3,076	0.815
Other Asia	2,384	-2.96 (-6.11)	0.3 (0.51)	3,176.16 (3.48)	-	3,283	0.907
Iran ^c	3,096	-0.4 (-0.47)	-1.51 (-0.12)	3,700.51 (0.09)	-	3,096	0.082
Arabian Peninsula ^d	2,519	-0.03 (-2.05)	-1.97 (-0.98)	8,793.33 (0.56)	-	3,099	0.332
Upper Middle East ^c	3,107	0.31 (0.69)	-3.83 (-0.63)	2,007.85 (0.17)	-	3,009	0.127
Turkey ^c	3,328	-7.38 (-2.69)	13.41 (2.28)	396.96 (2.76)	-	3,328	0.885
North Africa	3,231	-7.82 (-11.44)	8.85 (9.9)	1,137.69 (28.22)	-	3,233	0.988
South Africa ^a	2,962	-2.64 (-1.94)	3.73 (0.65)	2,291.49 (0.31)	542 (0.07)	2,833	0.632
South East Africa	2,053	-5.3 (-0.53)	2.03 (0.36)	1,512.13 (0.99)	-	3,061	0.577
Other S.S.Africa ^d	2,354	1.76 (2.05)	-1.19 (-1.5)	3,281.28 (1.6)	-	3,435	0.434
Mexico	2,895	-0.61 (-4.64)	0.71 (0.53)	3,025.23 (1.44)	-	3,280	0.969
Brazil	3,146	-3.16 (-7.52)	10.05 (7.3)	890.16 (33.73)	-	3,235	0.947
Paraguay, Uruguay, Argentina	2,901	0.77 (1.05)	-5.33 (-1.85)	-259.2 (-0.69)	-	2,950	0.348
Other South America	2,535	-3.01 (-4.94)	7.91 (4.46)	846.96 (10.26)	-	2,868	0.918
Russia ^c	3,118	-2.31 (-12.12)	1.77 (0.42)	1,831.82 (0.35)	-	3,118	0.795
Annex I of FUSSR ^c	3,047	-8.97 (-1.71)	5.07 (2.15)	3,390.46 (0.23)	-	3,047	0.731
Other FUSSR ^d	2,553	4.74 (0.22)	-1.22 (-0.11)	418.2 (5.29)	-	2,884	0.171
Eastern Europe	3,259	2.18 (0.35)	-4.81 (-0.4)	-20.59 (-0.74)	-	3,257	0.255

Values in parenthesis indicate t-statistic

^a Saturation level is estimated based on food consumption statistics

^b Canada's saturation value is set to the US level

^c Current consumption level exceeds the given saturation level

^d Sign condition of per capita GDP parameter is not satisfied

the past 20 years, so we consider them to have already been saturated. Saturation parameters are assigned to the other regional models based on the similarity of the food share. We used the Consumption Similarity Index [37] to quantify the similarity of the current share. As a result, the US parameter was assigned to Canada, the Western Europe parameter was assigned to Oceania and Argentina, and the Japanese parameter was assigned to the other regions. With these saturation parameters, the other growth model

parameters are estimated based on the data of each region in the same way as the total energy model estimation. The absolute estimation error for each region in 2003 falls in the range 0.0–3.0 %; on average, it is 0.7 %.

The item share within the food class is fixed to the 2000–2003 average for each region. Multiplying the regional population, dietary energy consumption per capita, share of food class, and share of food item, the demand for each food item is calculated. It should be noted that our energy

Table 3 Food demand function estimation results (reduced GINI scenario)

Region names	Average consumption (kcal/day)	β_1	β_2	β_3	β_4	Saturation level (kcal/day)	Correlation
USA ^a	3,754	-0.19 (-7.15)	4.96 (7.29)	1,176.44 (10.06)	2,765 (48.71)	3,941	0.994
Canada ^b	3,605	-0.47 (-10.98)	10.33 (11.01)	1,036.61 (50.88)	(-)	3,941	0.964
Western Europe ^a	3,536	-0.09 (-1.67)	0.71 (0.54)	1,633.2 (1.39)	2,205 (2.31)	3,838	0.983
Japan ^a	2,768	-0.11 (-0.35)	-0.21 (-0.01)	1,240.77 (0.07)	1,583 (0.09)	2,824	0.952
Oceania ^c	3,114	0 (0.36)	-3.83 (-1.98)	-24,592.36 (-0.53)	-	2,547	0.058
China	2,940	-12.26 (-2.75)	1.78 (1.04)	1,378.17 (1.96)	-	2,672	0.972
Mongolia, DPRK	2,185	-4.42 (-1.1)	2.42 (0.74)	596.57 (2.42)	-	2,613	0.216
Cambodia, Laos, Viet Nam	2,530	-17.69 (-5.29)	5.12 (3.97)	508.4 (7.42)	-	2,513	0.974
South Korea ^c	3,035	8.13 (1.92)	-16.32 (-1.99)	-343.09 (-10.71)	-	2,672	0.937
Malaysia, Singapore, Brunei ^c	2,867	1.63 (5.37)	-5.41 (-6.11)	-323.86 (-15.46)	-	2,547	0.935
Indonesia	2,891	-14.72 (-3.21)	5.12 (2.45)	844.67 (5.64)	-	2,545	0.965
Thailand	2,424	-0.55 (-5.73)	-1.78 (-0.99)	4,349.26 (0.64)	-	2,601	0.845
Philippines	2,480	-11.11 (-4.76)	9.19 (4.13)	812.81 (8.1)	-	2,461	0.911
India	2,473	-12.85 (-3.22)	2.63 (1.48)	908.85 (2.07)	-	2,489	0.931
Afghanistan, Pakistan	2,316	-6.76 (-7.01)	-0.94 (-0.76)	5,823.78 (0.93)	-	2,461	0.860
Other Asia	2,384	-8.82 (-10.87)	0.49 (0.96)	2,985.77 (3.04)	-	2,484	0.928
Iran ^c	3,096	16.64 (1.15)	-20.72 (-1.12)	-214.75 (-3.11)	-	2,545	0.374
Arabian Peninsula ^d	2,519	-0.19 (-2.55)	-2.51 (-1.4)	10,851.41 (0.6)	-	2,518	0.497
Upper Middle East ^c	3,107	-1.3 (-0.78)	8.45 (0.77)	-316.41 (-2.58)	-	2,550	0.164
Turkey ^c	3,328	4.28 (6.63)	-7.38 (-6.42)	-733.3 (-32.2)	-	2,700	0.895
North Africa	3,231	20.36 (2.19)	-25.77 (-2.18)	-625.37 (-7.09)	-	2,581	0.952
South Africa ^c	2,962	-2.64 (-1.94)	3.73 (0.65)	2,291.49 (0.31)	542 (0.07)	2,833	0.632
South East Africa	2,053	-8.47 (-0.97)	1.98 (0.44)	814.41 (0.81)	-	2,430	0.562
Other S.S.Africa ^c	2,354	6.1 (3.1)	-4.97 (-3.37)	3,751.79 (0.71)	-	2,470	0.466
Mexico	2,895	6.91 (2.24)	-24.32 (-2.28)	-279.31 (-7.34)	-	2,575	0.931
Brazil	3,146	5.3 (1.28)	-18.78 (-1.84)	-1,100.37(-0.35)	-	2,601	0.877
Paraguay, Uruguay, Argentina	2,901	0.31 (0.24)	-1.41 (-1.45)	-655.55 (-0.36)	-	2,642	0.350
Other South America	2,535	-7.12 (-5.43)	17.34 (5.11)	405.67 (10.71)	-	2,532	0.913
Russia ^c	3,118	5.15 (1.43)	-8.55 (-1.57)	-328.7 (-3.53)	-	2,742	0.802
Annex I of FUSSR ^c	3,047	3.07 (0.91)	-4.47 (-5.74)	-1,138.67 (-0.37)	-	2,728	0.844
Other FUSSR ^d	2,553	6 (0.24)	-2.84 (-0.21)	176.53 (24.71)	-	2,653	0.166
Eastern Europe	3,259	4.93 (1.96)	-7.14 (-1.69)	-516.55 (-30.57)	-	2,766	0.421

Values in parenthesis indicate t-statistic

^a Saturation level is estimated based on food consumption statistics

^b Canada's saturation value is set to the US value

^c Current consumption level exceeds the given saturation level

^d Sign condition of per capita GDP parameter is not satisfied

consumption model and food class share estimation model are explained only by per-capita GDP and do not depend on the price of food.

5 Results

Using this framework and scenarios, we estimated food demand/production, area of agricultural land use, and yield

from 2000 to 2100 for every 10 years. In total, simulations for eight scenarios were carried out for a combination of the following cases: expected and low growth for agrotechnologies; fixed and reduced GINI for food access disparity; and B2 climate and 1990 fixed climate. Under all scenarios, an agricultural land use pattern was obtained that satisfied global food demand throughout the study period. For simplicity, we set a base scenario, taking low technological growth, fixed GINI, and B2 climate, which requires

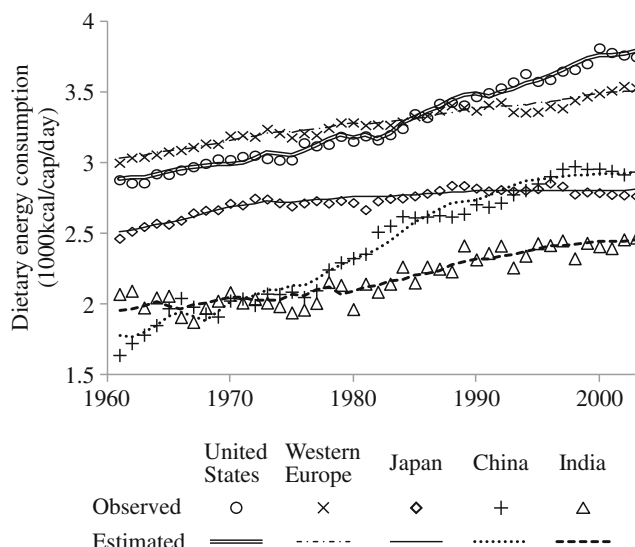


Fig. 10 Observed and estimated dietary energy consumption for five selected regions

maximum agro-land use, and examined the impacts of alternative scenarios compared with this base scenario.

First, the global dietary energy consumption under the two demand scenarios is shown in Fig. 12. Total energy demand increases by 96 % in the fixed GINI scenario and 58 % in the reduced GINI scenario between 2000 and 2100. During this period, the population increases by 67 % in the B2 scenario. As a result, the dietary energy consumption per capita increases by 17 % in the former and decreases by 5 % in the latter, even though per-capita GDP increases by 440 % in both scenarios. In this study, we assume that chronic malnutrition is eliminated when the prevalence is less than 5 %, and the gap reduction in food access will contribute to eliminating malnutrition with less total food supply. The result presented in Fig. 12 indicates that the promotion of equity in food access has a substantial impact on food demand. Compared with the fixed GINI scenario,

the total dietary energy consumption of the reduced GINI scenario is 20 % smaller.

This figure also shows the composition of food class. Reflecting the economic growth, the share of animal products, vegetable oils, and sugar is projected to increase. This change in food class composition may require more agricultural land than that for vegetable product-dominant composition.

Second, the total area of agricultural land use for all crops and average yield for wheat for four selected scenarios are shown in Fig. 13. In 2000, the estimated agro-land area was 3 % smaller than that in the statistics. It should be noted that all food is assumed to be generated from the eight crops in this study; therefore, the estimated geographical distribution of the crop harvest grid must differ from the actual distribution, and some regions such as Mexico and Mongolia have low accuracy in the estimation even though the global estimation error is quite accurate. In this sense, this estimation is not a prediction that considers real regional variety or constraints in production or trade but is representative of a possible land-use pattern to meet the assumed demand.

The base scenario, depicted by the solid line, projects that the area of agricultural land used for wheat production increases by 18 % from 2000 to 2030, then decreases. In 2100, the area is reduced from that of 2000 by 13 %. Even though food energy demand increases significantly, as shown in Fig. 12, the yield increase by the assumed technological progress exceeds the demand increase after 2030 in this scenario.

In the case of a fixed climate, climate change is completely mitigated. The trend is quite similar to that of the base scenario but projects an approximately 3 % smaller area in 2100 than the base scenario projection. This means that the climate change in the B2 scenario, in which the global average temperature is expected to increase by approximately 2.6 °C in 2100 from the 1990 level, has a negative effect on agricultural productivity and requires that the agricultural land area increases to meet the demand. Looking at the average yield

Fig. 11 Two scenarios of the average dietary energy consumption for seven selected regions (*right* fixed GINI scenario, *left* reduced GINI scenario)

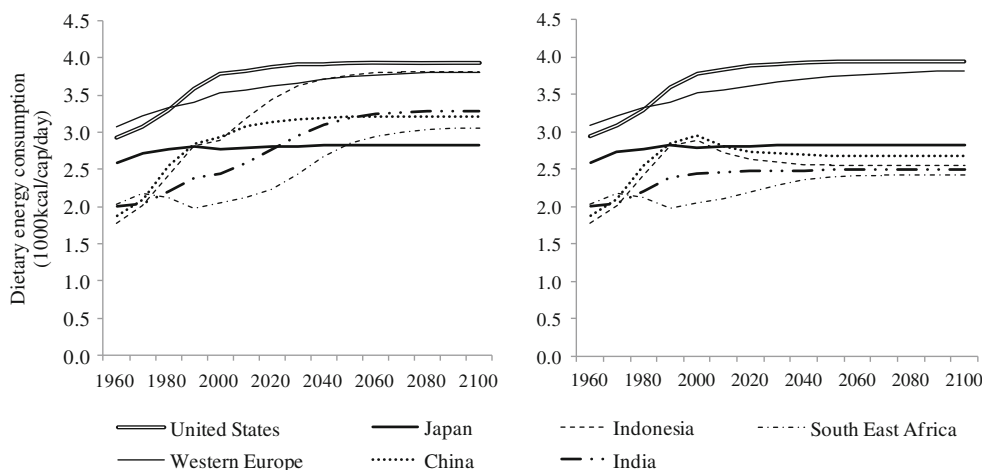
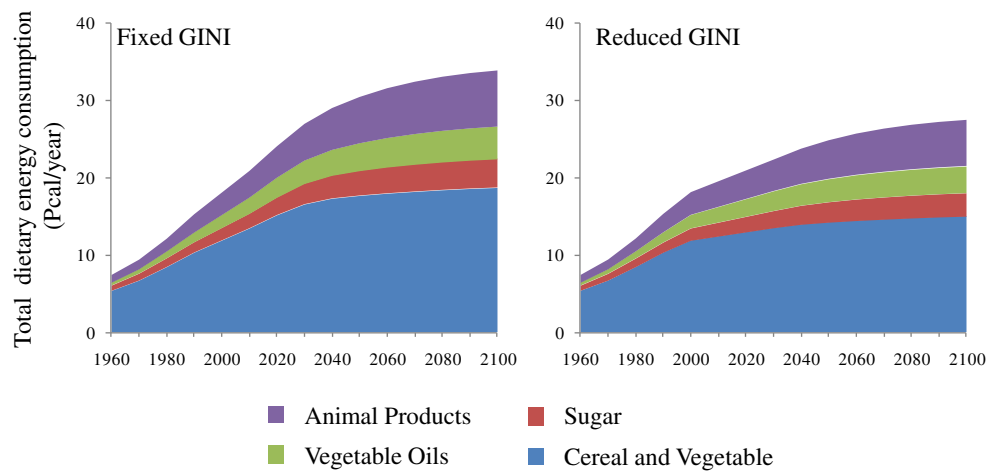


Fig. 12 Global dietary energy consumption of four food classes in fixed and reduced GINI scenarios



of wheat, the fixed climate scenario has a higher path than the base scenario; it is 10 % higher in 2100.

Both the expected technology scenario and the reduced GINI scenario project a constant decline in the required agricultural land area. During the period between 2000 and 2100, it is reduced by 47 and 39 % in these scenarios, respectively. A reduction of disparity in food access affects the land area immediately through a decline in the per-capita energy demand in developing countries, as shown in Fig. 11. Looking at the average yield of wheat, the reduced GINI scenario marks a higher yield than the base scenario through the analysis period; it is 6 % higher in 2100. Even though the agricultural technology progress path is the same in these scenarios, the smaller demand makes the average yield higher because the harvesting grid is allocated by priority of production value in this study. In other words, smaller demand only needs more productive grids. In contrast, larger demand requires an expansion of the harvesting area to land less suitable for agriculture.

The expected technology scenario gives the highest world-average yield among the chosen scenarios for wheat. Technological progress increases the yield, and higher yield needs a smaller harvested area to meet the demand, which

again leads to higher yield. Because of this assumed increase in technological progress and yield, despite the increase in demand and shift caused by an increase in population and per-capita GDP, the agricultural land area satisfying the demand declines.

In summary, the prospects of food access disparity and agrotechnological progress have a significant impact on the projection of food availability, agricultural land use, and productivity—no less than that of climate change. Based on the results of our scenario analyses, technological progress and the promotion of equitable food access are estimated to have sufficient potential to alleviate the negative impact of climate change on food security.

The above results are for the global average. However, the impacts of climate change are considered to differ by region, and how agriculture performs against climate change is one of our concerns, especially in developing countries. Figure 14 shows agricultural land use taking the cases of four regions: Western Europe, China, India, and South East Africa. In Western Europe and China, the figure indicates that the fixed climate scenario requires larger area for agriculture in total. This means that the assumed global

Fig. 13 Estimated global agricultural land area and global average yield of wheat

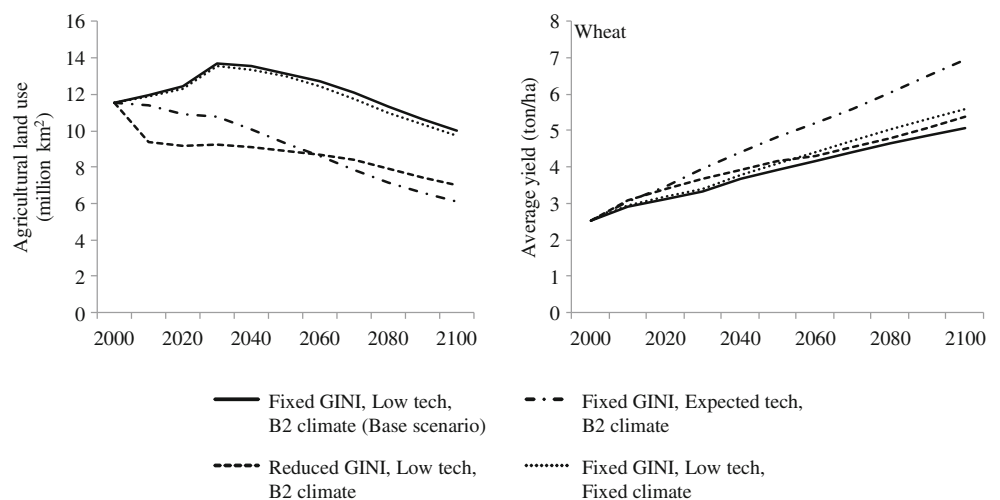
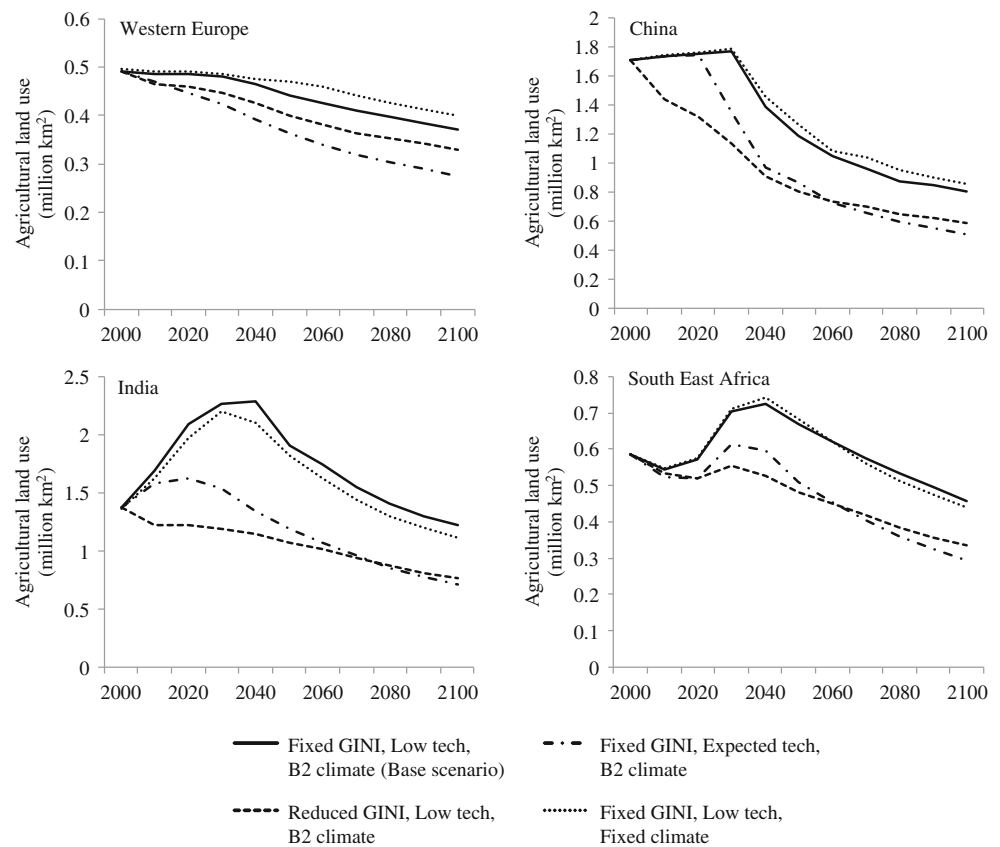


Fig. 14 Agricultural land use in Western Europe, China, India, and South East Africa



warming will have a positive impact in these two regions where substantial land at higher latitude is used for agriculture even though the climate impacts vary among crops and locations within the regions; some crops in the same location gain from climate change, but others may lose. In India, the fixed climate scenario needs less land than the base scenario; in other words, climate change will have negative impact on agriculture. In South East Africa, the base and fixed climate scenarios have almost the same path in agricultural land use, but climate change is expected to have a negative effect in the long term.

Both the expected technology scenario and the reduced GINI scenario require a smaller land area for agriculture in all regions. Even though the dietary energy consumption distributions of the fixed and reduced GINI scenarios are identical in Western Europe, the equitable food access in developing countries requires lower export from Western Europe. This pushes down the agricultural land use there. In China, India, and South East Africa, the expected technology and reduced GINI scenarios need much less land use than the base and fixed climate scenarios. This means that the assumed technological progress and the promotion of equitable food access are estimated to have sufficient potential to alleviate the negative impact of climate change on food security in the currently relatively poor regions as well.

It should be noted these outcomes are under the assumption that the food imports in regions such as China, India,

and South East Africa will increase with future increases in the demand for animal and processed food. It is controversial whether these countries will increase their food imports or not. In most countries, employment in the agricultural sector is an important political issue, and sometimes they protect the domestic products from competitive imported products. In other cases, if they fail in economic growth and a massive increase of food imports is not affordable, they have to supply crops themselves. In this case, however, the presumed food demand scenario may be changed. If these regions do not increase their imports, the pathway of land use in the developing countries shown in Fig. 14 will be pushed up, while the pathway of exporter regions will be pushed down.

It should also be noted that various adaptation measures, such as changing the crop calendar and harvesting sites, cultivation, and flexible trade against land use constraints, are already incorporated in the base scenario. This means that the global agricultural system is assumed to be managed quite idealistically and that some component such as changing the cropping calendar would be realized in the short term, but another part such as agricultural trade would take time to be more fair and flexible because of political reasons in many countries. These results, in this sense, are representative of a possible future but are not predictive, considering all the barriers and inefficiencies in the real world.

6 Conclusions

In this study, the impact of agrotechnological progress and the reduction of food access disparity are demonstrated in comparison with climate change scenarios. Under the agrotechnology, food access, and climate change scenarios during the period between 2000 and 2100, crop yields, agricultural land use, and food demand were estimated using a new analytical framework that incorporates AEZ methodology and the global food demand-trade model. For the agroproductivity scenario development, we developed a calibration method to extract the agrotechnological factor contribution to crop yield from statistics and AEZ yield estimation. This agrotechnological factor contribution implicitly includes the historical trend of technological progress, land use constraint, and agricultural labor/capital conditions. Using the estimated agrotechnological factor and statistical data on yield, two scenarios of agrotechnological progress were generated. In addition, based on the definition of hunger by the FAO, two scenarios of food demand, in which different levels of food access disparity are assumed under the B2 socioeconomic scenario, were also generated taking food access disparity into consideration.

The results indicate that (1) the assumed agroproductivity progress will have a substantial impact on crop yields and agricultural land use in this century; (2) a reduction in food access disparity will reduce the total food demand significantly in developing countries, leading to a smaller required harvesting area; and (3) both of these factors, the progress of agroproductivity and the reduction in food access disparity, have no lesser impacts on agriculture than climate change, which has been considered to be a significant factor in food security in past studies.

The assumed climate change increases the total agricultural land use, which represents a negative impact of climate change on agriculture. The total area of agricultural land required to meet global food demand is estimated to decrease substantially in two scenarios: the expected technology scenario and the reduced GINI scenario. The former scenario increases productivity, and the latter scenario decreases the total food demand even though the prevalence of malnutrition is eliminated in both scenarios. This implies that the negative impact of climate change on food security could be recovered by agrotechnological progress and the alleviation of disparity. Our results suggest that these factors may play more important roles than climate change in future global food security.

In the scenario development, various simplifications or assumptions were employed. Agrotechnological progress was determined statistically and did not necessarily reflect any potential of the individual technologies in the future. In addition to our statistical approach, a bottom-up analysis

compiling the possible yield improvement by each technology/technique would be needed. To develop the reduced disparity scenario, we applied the minimum GINI index to the setting of the saturation level of average food demand for all regions in which the prevalence of malnutrition is more than 5%. This setting made the average dietary energy demand lower than the current level for some countries and malnutrition was eliminated. This indicates that this scenario may demonstrate the maximum impact of disparity reduction, and we should thus address a greater variety of disparity scenarios in future studies. Crop production for biofuels was omitted from this study. Increased demand for biofuels may affect agricultural land use and food security. Demand for energy crops should also be incorporated in future studies.

Acknowledgments This study has been conducted as part of the “ALPS” (alternative pathways towards sustainable development and climate stabilization) project, supported by the Ministry of Economy, Trade and Industry, Japan. This study is partly supported by KAKENHI (23760490).

Appendix I: IPCC SRES Scenarios

There are four basic scenarios in the SRES report: A1, A2, B1, and B2. With regard to the population prospects, there are only three different trajectories because scenarios A1 and B1 have the same population trajectory. These two scenarios assume a higher economic growth around the world and lower birth rates in developing countries. As a result, they have the lowest population trajectory of the scenarios. The A2 scenario assumes self-reliance regions, lower trade flows, and uneven economic growth. Reflecting international disparities, a higher birth rate in developing regions and the largest population among the scenarios is assumed. The B2 scenario describes intermediate economic growth and moderate population growth, and the fertility rates were assumed to converge to the same level as the UN 1998 medium scenario.

Appendix II: Feed Demand for Animal Production

In this study, we assumed four types of animal products: bovine meat, pig meat, poultry, and milk. Alexandratos [38] provides a simple equation to estimate the feed demand for animal production. However, the intensity of feeding varies significantly by region: in some regions, the products come from non-grain-fed animals, whereas other regions feed high-calorie cereals intensively. We assume that two feed intensity vectors, V_e and V_i , are the required feed for unit production of the various types of animal products in extensive and intensive feeding systems. Assuming a region-specific

parameter α , the regional feed demand Q is calculated using the following equation:

$$Q_f = ((1 - \alpha) \cdot V_e + \alpha \cdot V_i) \cdot X \quad (7)$$

where X is the production volume vector of animal products. V_e and V_i are assumed on the basis of Alexandratos' study and reports from agricultural experiments in Japan. Using the data of Q_f and X in 2000 from FAOSTAT, α is estimated for each region.

We also assume that the feed consists of the eight kinds of crops considered in the land use analysis in this study. The regional share of primary crops for feed is fixed to the value in 2000.

Appendix III: Food Trade Model

In this model, the regional food demand is satisfied by domestic and imported products. The share of domestic product S_D is calculated by a binary logit model using the domestic price P_D and import price P_I .

$$S_D = \frac{\exp(-\theta_{d1} \cdot P_D + \theta_{d0})}{\exp(-\theta_{d1} \cdot P_D + \theta_{d0}) + \exp(-\theta_{d1} \cdot (1 + \tau) \cdot P_I)} \quad (8)$$

where τ is the tariff rate, θ_{d1} is the scale parameter of the error term, and θ_{d0} is the dummy parameter for domestic product. This equation means that as the domestic price decreases or the import price increases, the domestic share becomes high. The model parameters are estimated for each food item and region. Using the share and demand for all regions, the global demand for imports is calculated. The export share of region j in the global market, which is denoted as S_{Ej} , is estimated by a multinomial logit model using the domestic prices of export regions P_{Dj} .

$$S_{Ej} = \frac{\exp(\theta_{e1} \cdot P_{Dj} + \theta_{ej})}{\sum_j \exp(\theta_{e1} \cdot P_{Dj} + \theta_{ej})} \quad (9)$$

where θ_{e1} is the scale parameter of the error term and θ_{ej} is the dummy parameter for region j . The model parameters are estimated by the following process. First, scale parameters are estimated by solving the following equation for θ_1 :

$$\sigma = -\frac{p_1/p_2}{Q_1/Q_2} \cdot \frac{d(Q_1/Q_2)}{d(p_1/p_2)} = \frac{p_1 \cdot p_2}{p_1 + p_2} \cdot \theta_1 \quad (10)$$

where σ is the elasticity of substitution given by GTAP [27], p_1 and p_2 are the prices of two competitive items, and Q_1 and Q_2 are the demand volume of the items. For the domestic share model, θ_{d1} can be estimated using domestic and import prices. For the export share model, we calculate θ_1 for all price combinations of two export regions and θ_{e1} is

determined as an average of them. Second, the dummy parameters θ_{d0} and θ_{ej} are estimated to represent the share in 2000 under the estimated scale parameters.

In this model, food trade depends only on the price and tariff rate. However, in this study, we fixed the prices of agricultural products at the 2000 level during the analysis period. Therefore, the share of domestic products and the export share in the global food market are also fixed to the share in 2000 if land shortage does not occur in the allocation process. If land shortage occurs, the shortage volume of production is reallocated through the export share model where the export regions are limited to regions with marginal land for cultivation.

References

1. Easterling, W. E., Aggarwal, P. K., Batima, P. K., Brander, M., Erda, L., Howden, S. M., Kirilenko, A., Morton, J., Soussana, J.-F., Schmidhuber, J., & Tubiello, F. N. (2007). Food, fibre and forest products. Climate change 2007: impacts, adaptation and vulnerability. In M. L. Parry, O. F. Canziani, J. P. Palutikof, P. J. van der Linden, & C. E. Hanson (Eds.), *Contribution of Working Group II to the Fourth Assessment Report of the Intergovernmental Panel on Climate Change* (pp. 273–313). Cambridge: Cambridge University Press.
2. Nelson, G.C., Rosegrant, M.W., Koo, J., Robertson, R., Sulser, T., Zhu, T., Ringler, C., Msangi, S., Palazzo, A., Batka, M., Magalhaes, M., Valmonte-Santos, R., Ewing, M., Lee, D. (2009). *Climate Change: Impact on Agriculture and Costs of Adaptation*. International Food Policy Research Institute. <http://www.ifpri.org/publication/climate-change-impact-agriculture-and-costs-adaptation>. Accessed 8 Mar 2011.
3. IPCC (2000). *Special Report on Emissions Scenarios: A Special Report of Working Group III of the Intergovernmental Panel on Climate Change*. Cambridge University Press.
4. Rosegrant, M. W., Msangi, S., Ringler, C., Sulser, T. B., Zhu, T., and Cline, S. A. (2008). *International Model for Policy Analysis of Agricultural Commodities and Trade (IMPACT): Model description*. International Food Policy Research Institute.
5. Jones, J. W., Hoogenboom, G., Porter, C. H., Boote, K. J., Batchelor, W. D., Hunt, L. A., Wilkens, P. W., Singh, U., Gijsman, A. J., & Ritchie, J. T. (2003). The DSSAT cropping system model. *European Journal of Agronomy*, 18, 235–265.
6. Fischer, G., Shah, M., Tubiello, F. N., & van Velthuizen, H. (2005). Socio-economic and climate change impacts on agriculture: an integrated assessment, 1990–2080. *Philosophical Transactions of the Royal Society*, B, 360, 2067–2083.
7. Fischer, G., van Velthuizen, H., Shah, M., Nachtergaele, F.O. (2002). *Global agro-ecological assessment for agriculture in the 21st century: methodology and results*. IIASA RR-02-02, Laxenburg, Austria.
8. Fischer, G., Frohberg, K., Keyzer, M. A., & Parikh, K. S. (1988). *Linked national models: a tool for international policy analysis*. Netherlands: Kluwer Academic.
9. Tubiello, F. N., & Fischer, G. (2007). Reducing climate change impacts on agriculture: global and regional effects of mitigation, 2000–2080. *Technological Forecasting and Social Change*, 74, 1030–1056.
10. Grubler, A., O'Neill, B., Riahi, K., Chirkov, V., Goujon, A., Kolp, P., Prommer, I., & Slenetoe, E. (2007). Regional, national and spatially

- explicit scenarios of demographic and economic change based on SRES. *Technological Forecasting and Social Change*, 74, 980–1029.
11. Beddington, J. (2010). Food security: contributions from science to a new and greener revolution. *Philosophical Transactions of the Royal Society, B*, 365, 61–71.
 12. FAO (2009). FAOSTAT, Statistical Database of the United Nations Food and Agricultural Organization, <http://faostat.fao.org/site/0/Default.aspx>. Accessed 1 Nov 2009.
 13. Wise, M., Calvin, K., Thomson, A., Clarke, L., Bond-Lamberty, B., Sands, R., Smith, S. J., Janetos, A., & Edmonds, J. (2009). Implications of Limiting CO₂ Concentrations for Land Use and Energy. *Science*, 324(5931), 1183–1186.
 14. Gregory, P. J., Ingram, J. S. I., & Brklacich, M. (2005). Climate change and food security. *Philosophical Transactions of the Royal Society, B*, 360, 2139–2148.
 15. Ericksen, P. J., Ingram, J. S. I., & Liverman, D. M. (2009). Food security and global environmental change: emerging challenges. *Environmental Science & Policy*, 12(4), 373–377.
 16. Schmidhuber, J., & Tubiello, F. N. (2007). Global food security under climate change. *Proceedings of the National Academy of Sciences of the United States of America*, 104(50), 19703–19708.
 17. FAO (2006). *World Agriculture: Toward 2030/2050, Interim Report*. Food and Agriculture Organization of the United Nations.
 18. Ben-Akiva, M. and Lerman M. (1985). *Discrete Choice Analysis: Theory and Application to Travel Demand*, The MIT Press.
 19. U.S. Geological Survey (2008). *Global Land Cover Characteristics Data Base Version 2.0*, United States Department of the Interior, U.S. Geological Survey, Earth Resources Observation and Science Center. <http://eros.usgs.gov/Home>. Accessed 1 Nov 2009.
 20. Balat, M., & Balat, H. (2009). Recent trends in global production and utilization of bio-ethanol fuel. *Applied Energy*, 86, 2273–2282.
 21. The Royal Society (2008). *Sustainable biofuels: prospects and challenges*. Policy document 01/08, London.
 22. Seelke C.R., Yacobucci B.D. (2007). *Ethanol and other biofuels: potential for US–Brazil energy cooperation*. CRS Report for Congress, Order Code RL34191, Washington, DC.
 23. Jull C, Redondo P.C, Mosoti V, Vapnek J. (2007). *Recent trends in the law and policy of bioenergy production, promotion and use*. Legislative Study 95, Food and Agriculture Organization of the United Nations, FAO, Rome.
 24. Klijn, J.A., Vullings, L.A.E., van den Berg, M., van Meijl, H., van Lammeren, R., van Rheenen, T., Veldkamp, A., and Verburg, P.H. (2005). The EURURALIS study: technical document. Alterra-rapport 1196., Alterra, Wageningen.
 25. Lee, H.-L., Hertel, T.W., Sohngen, B., & Ramankutty, N. (2005). towards an integrated land use database for assessing the potential for greenhouse gas mitigation. GTAP Technical Paper 25.
 26. Ronneberger, K., Berritella, M., Bosello, F., and Tol, R.S.J. (2008). KLUM@GTAP: spatially-explicit, biophysical land use in a computable general equilibrium model, GTAP Working Paper No. 50
 27. Hartel, T. W. (1997). *Global trade analysis: modeling and applications*. New York: Cambridge University Press.
 28. Becker, J. J., Sandwell, D. T., Smith, W. H. F., Braud, J., Binder, B., Depner, J., Fabre, D., Factor, J., Ingalls, S., Kim, S.-H., Ladner, R., Marks, K., Nelson, S., Pharaoh, A., Trimmer, R., Von Rosenberg, J., Wallace, G., & Weatherall, P. (2009). Global bathymetry and elevation data at 30 arc seconds resolution: SRTM30_PLUS. *Marine Geodesy*, 32(4), 355–371.
 29. University of East Anglia Climate Research Unit (2008). *CRU Datasets*, British Atmospheric Data Centre. <http://www.cru.uea.ac.uk/cru/data/hrg.htm>, Accessed 1 Nov 2009.
 30. Hayashi, A., Akimoto, K., Sano, F., Mori, S., & Tomoda, T. (2009). Evaluation of global warming impacts for different levels of stabilization as a step toward determination of the long-term stabilization target. *Climatic Change*, 98(2), 87–112.
 31. Meehl, G. A., Covey, C., Delworth, T., Latif, M., McAvaney, B., Mitchell, J. F. B., Stouffer, R. J., & Taylor, K. E. (2007). The WCRP CMIP3 multi-model dataset: a new era in climate change research. *Bulletin of the American Meteorological Society*, 88, 1383–1394.
 32. FAO (2002). *AQUASTAT database*, Food and Agriculture Organization, Water Resources Development and Management Service. <http://www.fao.org/nr/water/aquastat/dbases/index.stm>, Accessed 1 Nov 2009.
 33. FAO Statistics Division (2008). *FAO Methodology for the Measurement of Food Deprivation, Updating the minimum dietary energy requirements*, http://www.fao.org/fileadmin/templates/ess/documents/food_security_statistics/metadatas/undernourishment_methodology.pdf. Accessed 1 Nov 2009.
 34. FAO (2012). Food security methodology, <http://www.fao.org/economic/ess/ess-fs/fs-methods/fs-methods1/ru/>. Accessed 10 Apr 2012.
 35. Aitchison, J. and Brown, J. A. C. (1957). *The lognormal distribution*. Cambridge: Cambridge University Press
 36. FAO (2012). Food security data and definitions, <http://www.fao.org/economic/ess/ess-fs/fs-data/ess-fadata/en/>. Accessed 10 Apr 2012.
 37. FAO (2003). *World agriculture: towards 2015/2030—an FAO perspective*. Rome: Food and Agriculture Organization of the United Nations.
 38. Alexandratos, N. (1995). *World agriculture: towards 2010: an FAO study*. Rome: Food and Agriculture Organization of the United Nations.